

Chapter-3

3.1 Introduction

In the earlier part of this thesis I had demonstrated that core and linker histones follow distinct mechanisms of diffusion in the nuclei of living cells. My experiments indicated that the core histones are in a multimeric form, and the linker histones show a unique distinct interaction time scale with the chromatin fiber. Thus it became interesting to ask how the diffusion dynamics of the histone proteins would change under conditions of global changes in chromatin architecture. I explored this possibility under two very varied conditions – first by a chemically-induced global decondensation of the chromatin in cells in culture, and next in an organismal context, when large-scale changes come about in chromatin structure with the onset of zygotic transcription during the development of the fruit-fly (*Drosophila melanogaster*) embryo. The rationale for each of these cases is described in brief below.

Histone proteins are subjected to an enormous number of post-translational modifications, including acetylation, methylation, phosphorylation, ubiquitination etc. [1]. These modifications play a central role in regulating the structural compaction of the chromatin and hence global genome function. The majority of these post-translational marks occur on the amino and carboxy-terminal tails of histones. Several histone modification enzymes play a vital role in structural and functional modification of the chromatin fiber - these enzymes are classified into different families, like Histone-Acetyl-Transferases (HAT), Histone-deacetylases (HDAC), Histone-Methyl-Transferases (HMT), kinases etc. These modifications lead to recruitment of other non-histone proteins which further modify chromatin structure – for instance methylation of histone H3 at lysine 9 leads to recruitment of heterochromatin protein-1 (HP1), which directs formation of highly condensed, heterochromatin structures. Generally acetylation of histones H3 and H4 is associated with an up-regulation of transcription. This greater accessibility of sites embedded in the nucleosomal structure, results from a decompaction of the chromatin structure. Thus HATs and HDACs play a major

role in governing gene expression by tuning the acetylation pattern of the chromatin [2]. Inhibition of HDACs by small molecules like Trichostatin-A (TSA), Scriptaid, or Sodium butyrate leads to global decondensation of the chromatin due to widespread acetylation of the histone-tails.

The first part of this chapter describes my work on TSA-induced chromosomal decompaction and its effect on histone dynamics and the interaction with the chromatin fiber inside the HeLa cell nucleus. In this study, we explore the effect of TSA on the diffusive mobility of the core and linker histones and how chemical modifications on core and linker histone can alter the mobility of the individual histones and hence their interaction with the chromatin fiber. Using near-single molecule methods, we have found that the interaction timescale of the freely diffusing linker histone increases significantly in TSA-treated cells. However, the multimeric form of the freely diffusing core histones is maintained in TSA treated cell nucleus despite significant chromosomal decondensation.

Another context, in which large-scale changes naturally come about in chromatin architecture, is during embryonic development. Recent work on differentiation of embryonic stem cells into neuronal lineages [3, 4] indicates that chromatin structure appears to be plastic in undifferentiated cells, whereas the chromosome gets more well defined structure in the differentiated cell nuclei. Neuronal differentiation involves changes in gene expression and nuclear architecture as well as cellular-morphological changes like neurite extension and synapse formation. So it is expected that the ES cells must be plastic enough to accommodate such tissue specific rapid and substantial structural changes. The genome in pluripotent ES cells must be in a highly plastic state so as to have the capacity to enter a distinct differentiation pathway. Once differentiation is initiated, lineage specification occurs by the implementation of gene-expression programs that gives each cell type a unique transcriptional profile. The molecular mechanisms for self-renewal, maintenance of pluripotency and lineage specification are poorly understood. One of the likely key factors to successful regulation of differentiation might be the unique chromatin structure of

undifferentiated cells. It is becoming increasingly clear that chromatin structure is very important for the pluripotency, stem cell identity and the cell fate regulation and decision. Studies on the dynamics of different somatic and oocyte specific linker histones in oocytes and in ES cells during nucleus transfer suggest that oocyte-specific H1FOO binds chromatin more tightly than somatic linker histones [5]. It has also been shown that the maternally expressed histone B4 is replaced by somatic H1A during early *Xenopus* embryogenesis and that there is a reduction of linker histone dynamics after the replacement of maternally expressed B4 by the somatic linker histones [6]. These results clearly indicate the pivotal role of chromatin structure in regulating differentiation programs and hence importance of studying the diffusion dynamics of core and linker histones during the early stages of embryonic development when marked changes come about in chromatin architecture [7, 8].

In the latter half of this chapter, I describe my attempts to understand the role of histone dynamics before and after cellularization in the early stages of *Drosophila* embryogenesis. I have studied the histone dynamics in the early *Drosophila* embryo to define the adaptability in chromatin organization as cellularization proceeds. Here we have observed a significant exchange of core and linker histones before cellularization. This dynamics is found to be modulated as development proceeds.

3.2 Effect on core and linker histone dynamics in HDAC inhibitor treated cells due to chromosomal spreading.

3.2.1 Methods

Cell culture and reagents.

HeLa cells stably expressing H2B-EGFP and H1.5-EGFP, were grown in 5 % FBS in DMEM (GIBCO) and incubated in a carbon-di-oxide incubator. Cells were plated at a density of 200,000 cells per dish in 5% complete medium and left overnight for adherence. TSA (SIGMA) was reconstituted in DMSO and was further diluted in complete medium. TSA at doses ranging from 0 to 200ng/ml was added to cells for varying times viz. 12 hrs, 24 hrs and 48 hrs.

3.2.2 Results

3.2.2.1 FRAP of H1.5-EGFP in controlled and TSA treated cells

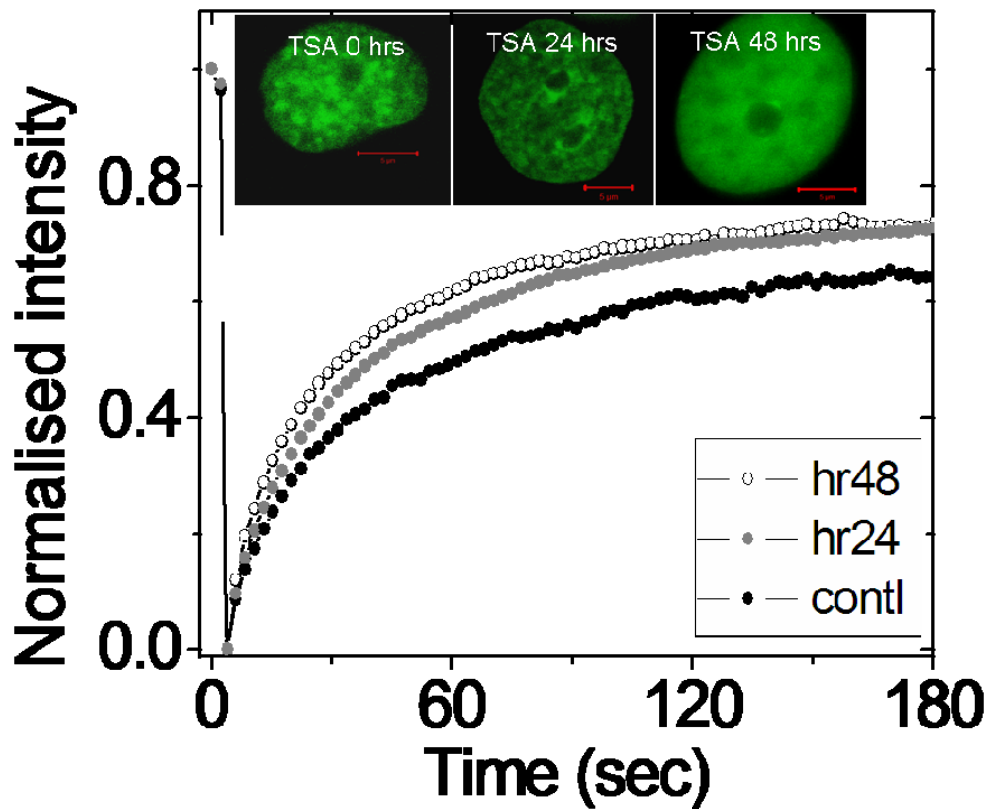
To understand the structural dependence of the chromatin fiber on interaction timescales of linker histones, we have carried out FRAP study upon TSA treatment of HeLa cells. From the literature we know that due to TSA treatment the euchromatin regions spread significantly and the size of the cell nucleus also increases due to de-condensed chromatin structure [9]. From a different study we have found that the expression of linker histones also increases significantly though the expression of core histones and non-interactive proteins, like EGFP, do not change. As the core and the linker histones are the major regulators of chromatin condensation, and the chemical modification of the core and linker histones can tune the structural stability of the chromatin fiber, it is important to understand the change in histone dynamics and the interaction of histone proteins due to TSA induced chemical modification of the core histones.

Our fluorescence recovery after photo-bleaching study shows significant higher recovery of the linker histones (H1.5-EGFP) in TSA-treated cells compared

to the control cells. In the **Figure 3.2.1** we have shown the higher fractional recovery of the linker histones (H1.5-EGFP) in different time points (control, 24 hrs, 48 hrs) after TSA treatment (100 ng/ml). We expect the higher fraction of fluorescence recovery in TSA treated cells is an effect of higher free fraction of the linker histones due to higher expression of linker histones. Due to 48 hrs of TSA treatment the expression level of linker histones increases significantly, though the binding sites on the chromatin fiber remain invariant, as a result we expect more free fraction of linker histones present in the photobleached region giving rise to a higher fractional recovery in the TSA treated cells than the control cells in normal physiological condition.

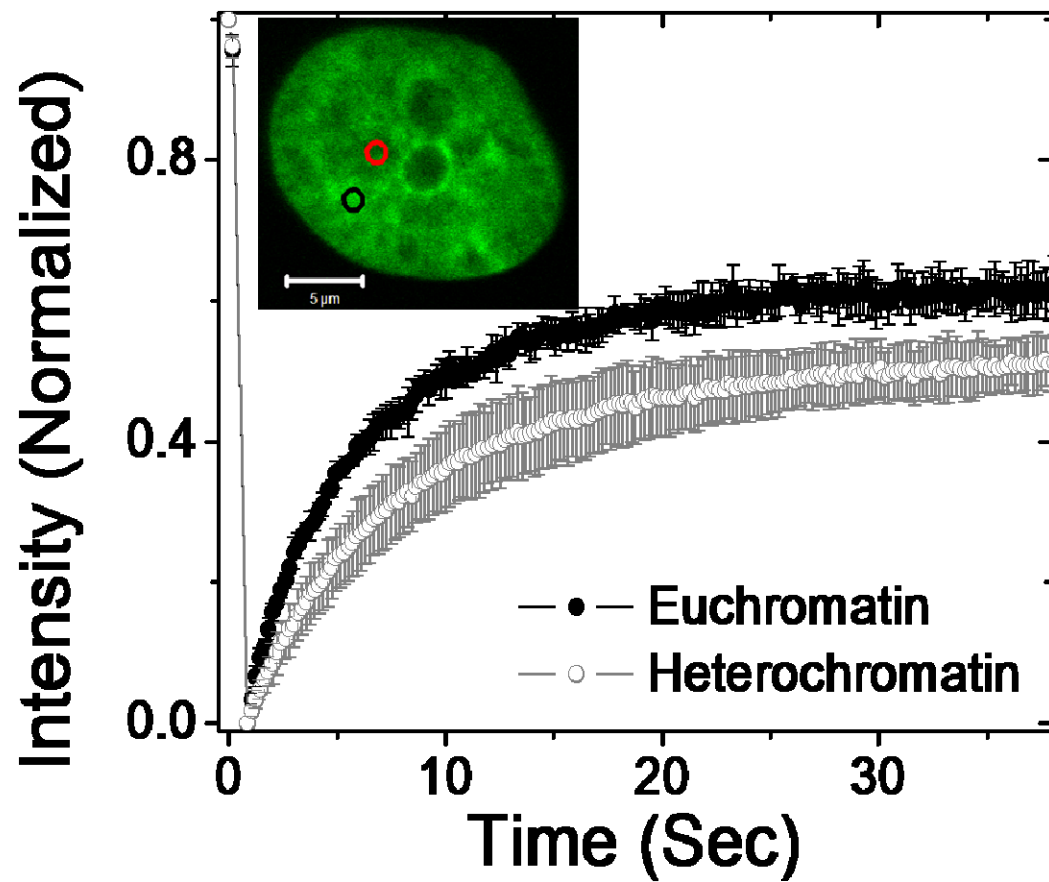
As TSA alters the euchromatin to heterochromatin fraction inside the cell nucleus, FRAP experiments are carried out in untreated cells to contrast the dynamics in these two regions in normal H1.5-EGFP expressing HeLa cell nuclei. Heterochromatin regions are more condensed than the euchromatin regions inside the cell nucleus. Heterochromatin regions are marked by methylated core histones and heterochromatin proteins (HP1). These heterochromatin proteins (HP1) are important for the higher order compacted chromatin structure. In the FRAP experiments, the area of photobleaching was adjusted such that the euchromatin and heterochromatin regions are not compromised. A higher fluorescence recovery was observed in the euchromatin regions compared to the heterochromatin regions for the HeLa nucleus expressing stable linker histones (H1.5-EGFP) as shown in the **figure 3.2.2**. Fluorescence recovery results indicate lower fractions of the freely diffusing linker histones in the more compact heterochromatin regions than the euchromatin regions.

Figure 3.2.1



Fluorescence recovery curves of linker histones (H1.5-EGFP) in different time-point (0 hrs, 24 hrs and 48 hrs) after TSA treatment (100ng/ml). Inset the confocal fluorescent images of the H1.5-EGFP expressing HeLa cells after the corresponding TSA treatment.

Figure 3.2.2



Linker histones (H1.5-EGFP) show significantly higher recovery in the euchromatin regions compared to the heterochromatin regions in HeLa cells under normal physiological condition.

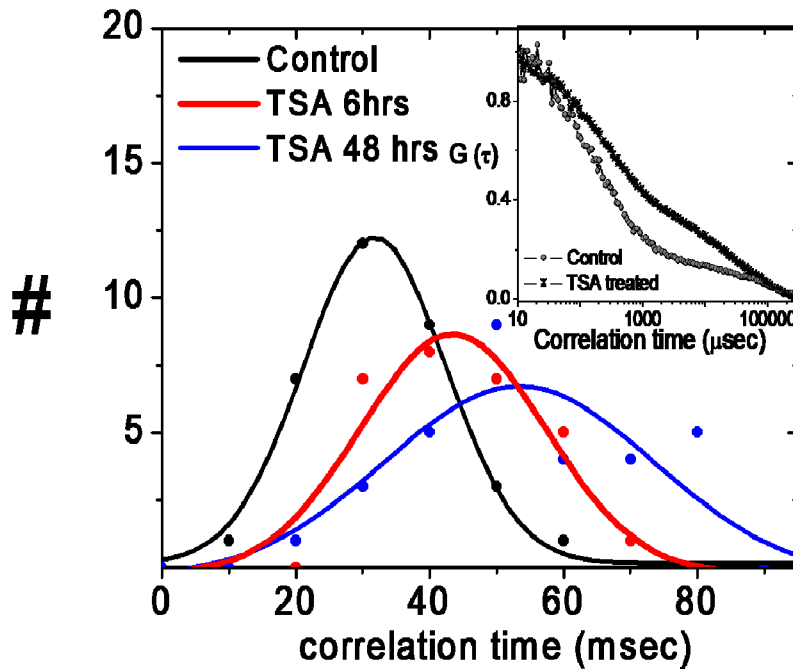
3.2.2.2 Mobility of linker histones (H1.5-EGFP) in TSA treated cells by FCS measurements.

Fluorescence correlation spectroscopy measurements are done to understand the diffusion behavior of the linker histones and to estimate the interaction timescales of linker histones in TSA treated cells compared to the control cells in normal physiological condition. Before FCS experiments photo-bleaching is performed to reduce the number of fluorescently tagged linker histones inside the confocal volume. FCS experiments are performed following the same procedure as I have described earlier. I observed a significant increase in interaction timescale for linker histone H1.5-EGFP in TSA treated cells compared to the control cells, as shown in **Figure 3.2.3**. TSA treatment at various time points (0 hr, 6 hrs, and 48 hrs) results in a subsequent increase in the interaction correlation timescale. From the literature we know the binding affinity of phosphorylated linker histones is significantly lower and it is observed that the phosphorylated linker histones are localized only in distinct patches in TSA treated cells compared to the control cells, where the distribution is almost uniform all over [10]. I expect this increased interaction timescales of H1.5-EGFP is an effect of both de-condensed chromatin structure and due to distinct localization of phosphorylated linker histones in the TSA treated cells.

To compare the interaction timescales of linker histones (H1.5-EGFP) in the euchromatin and heterochromatin regions, FCS experiments are carried out in untreated cells in these two regions in normal H1.5-EGFP expressing HeLa cell nuclei. As fluorescence recovery data depends upon many parameters it is difficult to estimate the interaction of the linker histones at the single molecular level, especially in a complex environment and in over-expressing H1.5-EGFP cells. Our FCS data indicates the mean interaction timescale in the euchromatin regions is similar compared to the mean interaction timescale for the heterochromatin regions as shown in the **figure- 3.2.4**. In heterochromatin regions of control cells the interaction timescale is $\sim (34 \pm 10)$ ms, whereas in the euchromatin regions the interaction timescale observed is $\sim (38 \pm 13)$ ms, as shown in **figure- 3.2.4**.

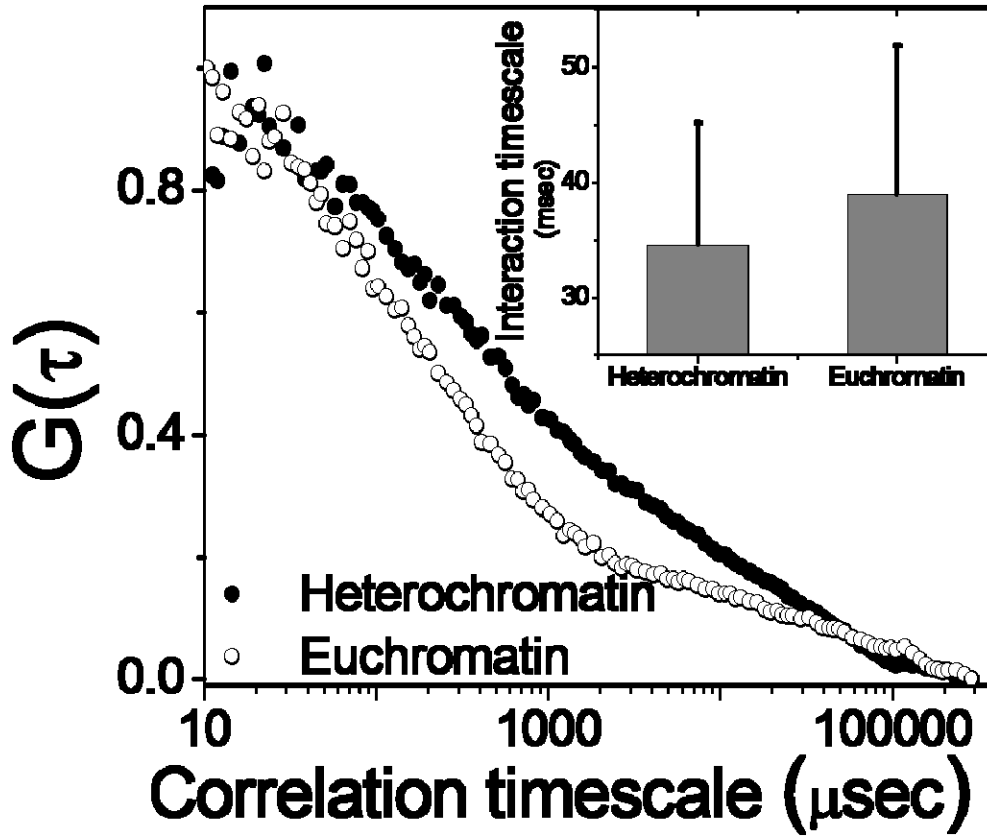
The fluorescence correlation spectroscopy data indicates though the heterochromatin regions are structurally more compacted than the euchromatin regions and different heterochromatin proteins (HP-1) are present in the heterochromatin regions to give it a structural stability, both the diffusion and the interaction timescales of the linker histones (H1.5-EGFP) are very similar in the euchromatin and heterochromatin regions.

Figure 3.2.3



Distribution of the interaction timescales of linker histones (H1.5-EGFP) at different time-points (0hrs, 6hrs, and 48hrs) of TSA treatment (100ng/ml), indicate a clear increase in interaction timescale upon TSA induced chromosomal spreading in HeLa cells. Inset, the corresponding FCS curves for H1.5-EGFP diffusion in control cells compared to the 48hrs of 100ng/ml TSA treated cells.

Figure 3.2.4



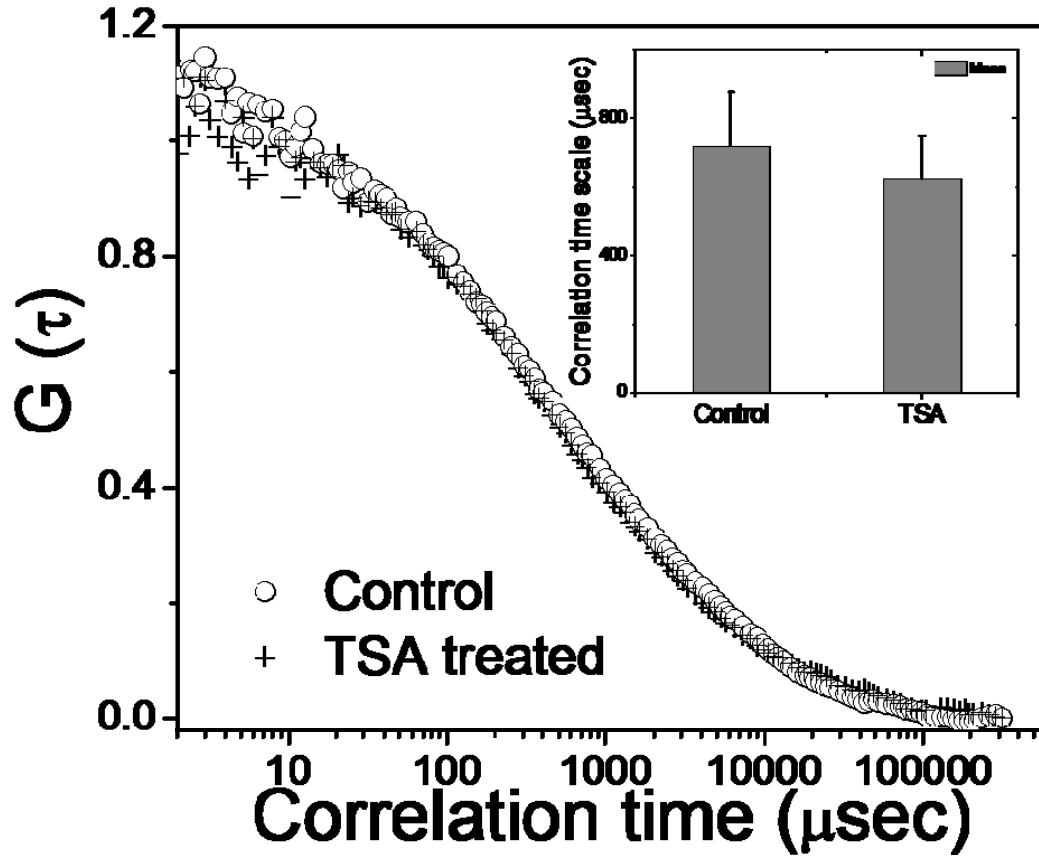
Fluorescence correlation spectroscopy curves of H1.5-EGFP in the euchromatin regions and heterochromatin regions HeLa cells in the normal physiological condition. In both cases there is a clear signature of interaction timescales. Inset, the mean interaction timescales of linker histones (H1.5-EGFP) in different euchromatin and heterochromatin regions.

3.1.2.3 Core histone mobility

From the fluorescent images, it is clear that the euchromatin region spreads significantly upon TSA treatment (48 hrs). Though the FRAP study of TSA treated H2B-EGFP cells show minimal recovery, like H2B-EGFP cells in normal physiological condition (Data not shown), it is interesting to see the diffusion mechanism of freely diffusing core histones in TSA treated cells. I have done fluorescence correlation spectroscopy study to check the monomeric–multimeric state of the freely diffusing core histones inside the cell nucleus. In the previous study [11] we have shown the core histones (H2B-EGFP/ H4-EGFP) are in multimeric form inside the HeLa cell nucleus, though in an over-expressing system in HeLa cell cytoplasm the core histones are in the monomeric form. This multimeric state of the core histones inside the cell nucleus is important to maintain the epigenetic state of the chromatin fiber. Using fluorescence correlation spectroscopic study, I have tried to check whether the multimeric form of the core histones, is maintained in the TSA treated HeLa cells. Instead of large spread in the correlation timescales, indicating the heterogeneity inside the cell nucleus, we can clearly see that the core histone diffusion timescale do not change significantly in the TSA treated cells compared to the control cells, as shown in **Figure-3.2.5**. Our fluorescence correlation study shows that the core histones are in the multimeric form in the nuclei of HeLa cells, treated with TSA for 48 hrs.

Our data clearly indicates that despite of higher expression of the linker histones and euchromatin spreading in the nucleus, the core histones are in multimeric form in the TSA treated cells.

Figure 3.2.5



FCS curves of H2B-EGFP diffusion in 48hrs of TSA treated (100ng/ml) cells compared with the control cells. Inset, the mean correlation timescale of H2B-EGFP diffusion in HeLa cells with and without TSA treatment.

3.3 Role of Histone dynamics during cellular differentiation in earlier state of *Drosophila* embryo development.

3.3.1 Results

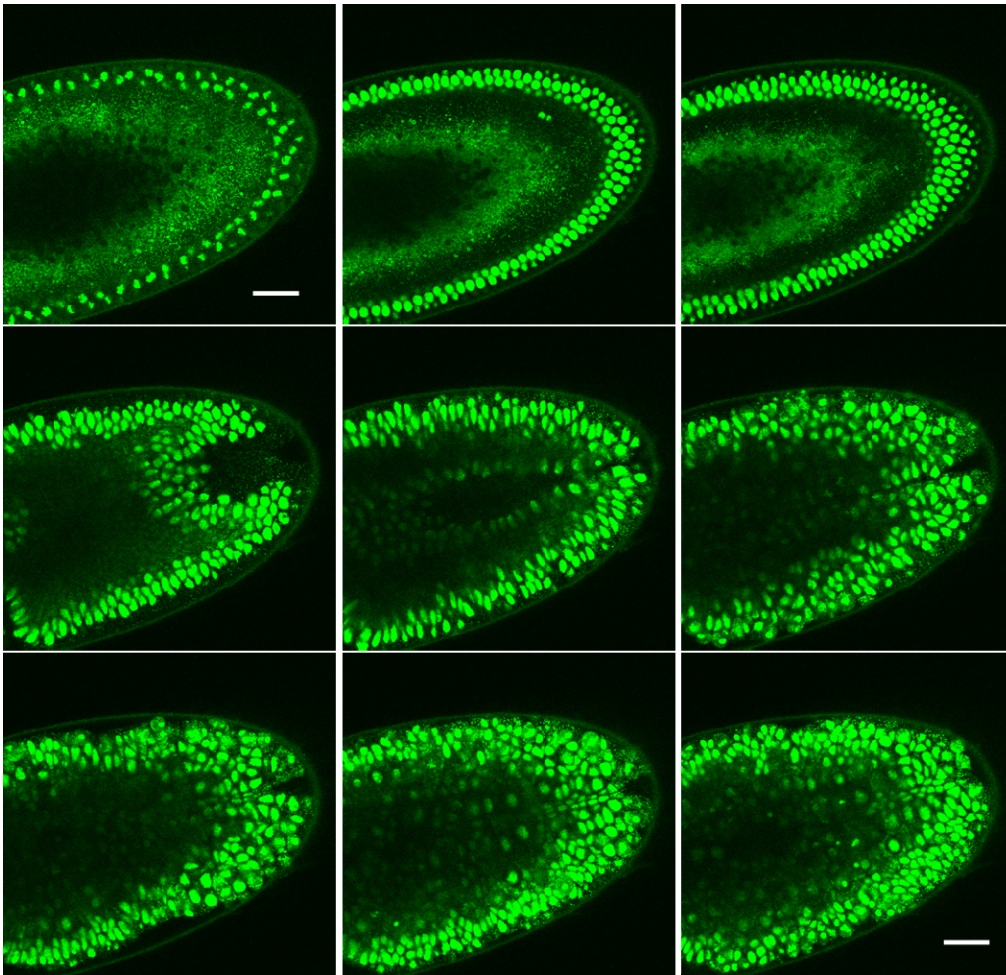
The model system used in our experiments is the embryo of *Drosophila melanogaster* where one of the core histones H2B is genetically tagged to EGFP (H2B-EGFP). To understand the role of linker histone dynamics before and after cellularization, Alexa-488 labeled linker histones (H1-Alexa488) were microinjected into the embryo in the very early stages of development (before 11th nuclear division) and the binding affinity of linker histones in different stages of embryogenesis was studied.

Confocal fluorescence microscopy has been used to visualize the chromosomal DNA and the nuclear localization inside a developing *Drosophila* embryo. **Figure-3.2.1-3.2.3**, show that the EGFP-tagged core histones precisely mark the cell nuclei and this histone labeling does not affect the nuclear division and embryonic development.

The anterior part of a developing fruit fly (*Drosophila melanogaster*) embryo is shown in **figure-3.2.1**. The images are taken at a depth of ~40 μm from the ventral surface (The scale bar ~20 μm). Total time taken is about 4 hours (though it strongly depends upon the temperature of the environment). The development of the anterior part is completely different from the development of the posterior part (**Figure-3.2.2**). In these figures, the anterior and posterior part of the embryo indicate the rapid nuclear division up to 14th mitotic cycle (13th nuclear division) followed by cellularization, asymmetric nuclear formation, differential chromosomal compaction and distinct nuclear localization.

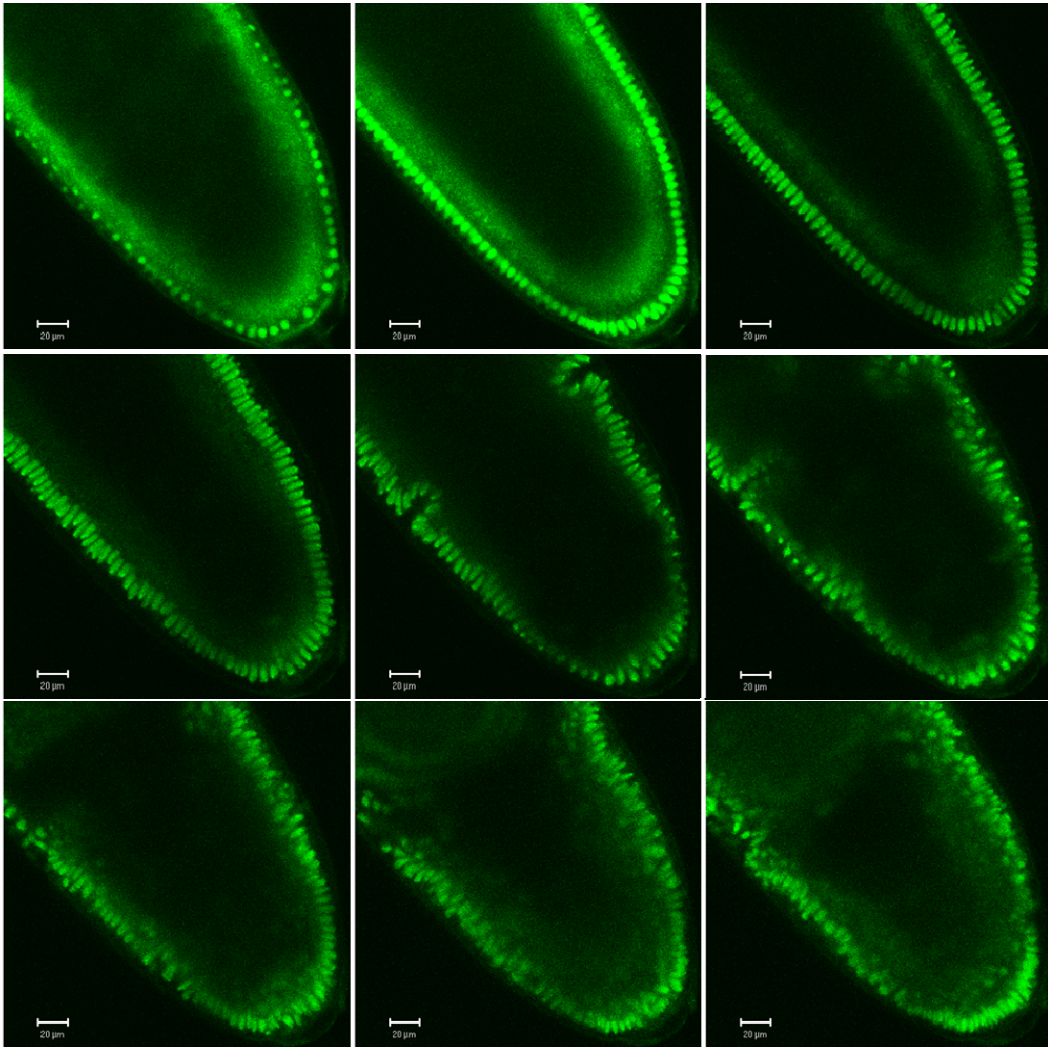
Figure-3.2.3 shows that the chromosomal compaction, chromosomal segregation and separate nuclear formation at the time of mitotic division. The real time fluorescent images of the embryonic development indicate that the fluorescence tagging of the core histones does not affect the developmental time frame of the fruit-fly embryo. Hence tracking the mobility of the core histones, genetically tagged with EGFP protein, has a physiological implication.

Figure 3.3.3.1



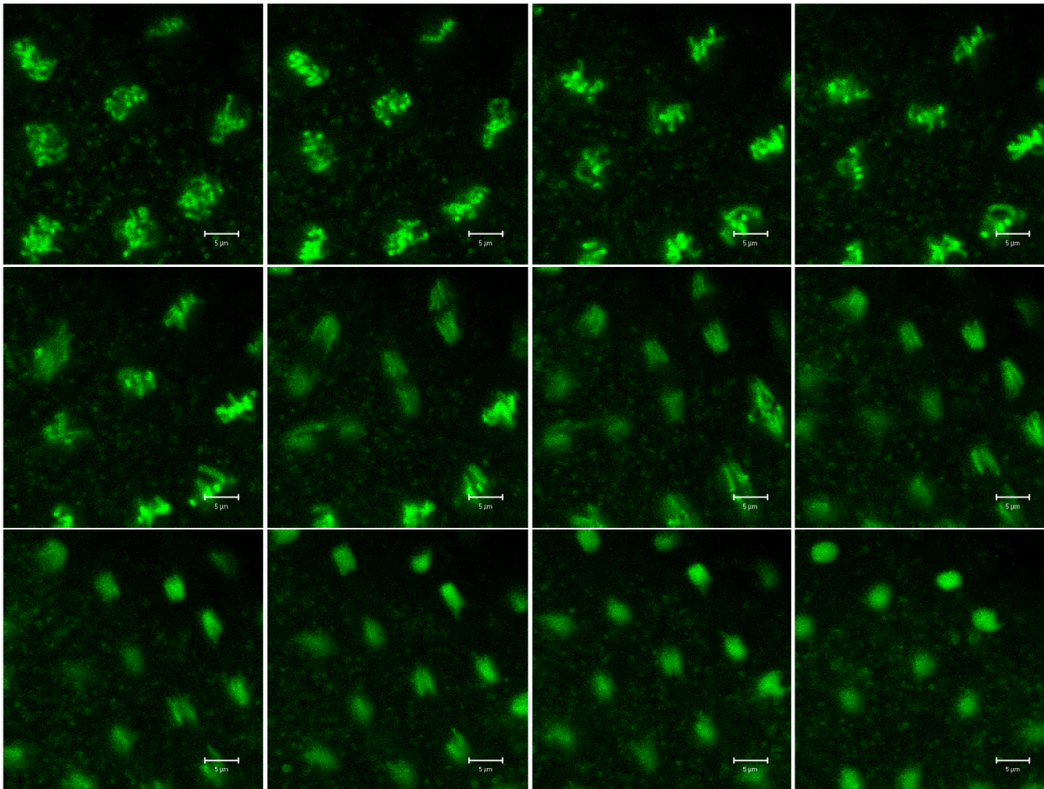
Different stages of development in the posterior part of the *Drosophila* embryo are shown in the figure. Here core histone (H2B) is fluorescently tagged with EGFP. Scale bar~20 μm .

Figure 3.3.3.2



Different stages of development in the anterior part of the *Drosophila* embryo are shown in the figure. Here core histone (H2B) is fluorescently tagged with EGFP. Scale bar~20 µm.

Figure 3.3.3.3

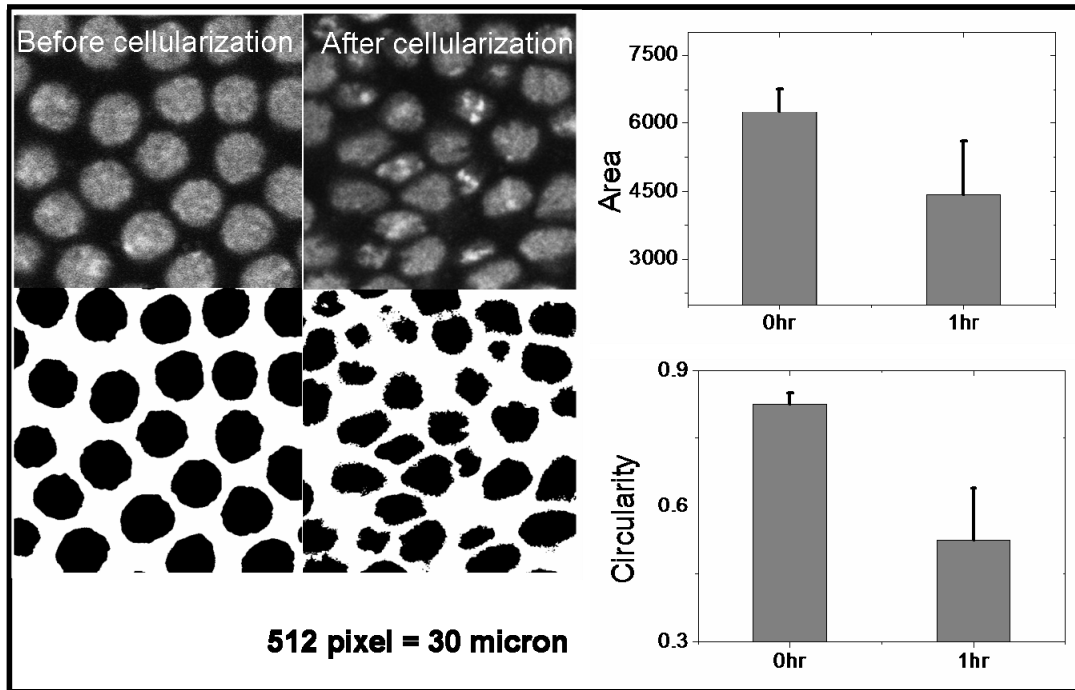


The 13th nuclear division in the posterior part of the *Drosophila* embryo is shown in the figure. Here the core histones (H2B) fluorescently tagged with EGFP, clearly indicate the chromosomal compaction and segregation at the time of mitotic division. Scale bar~5 μm.

3.3.1.1 Core histone dynamics before cellularization in the developing *Drosophila* embryo.

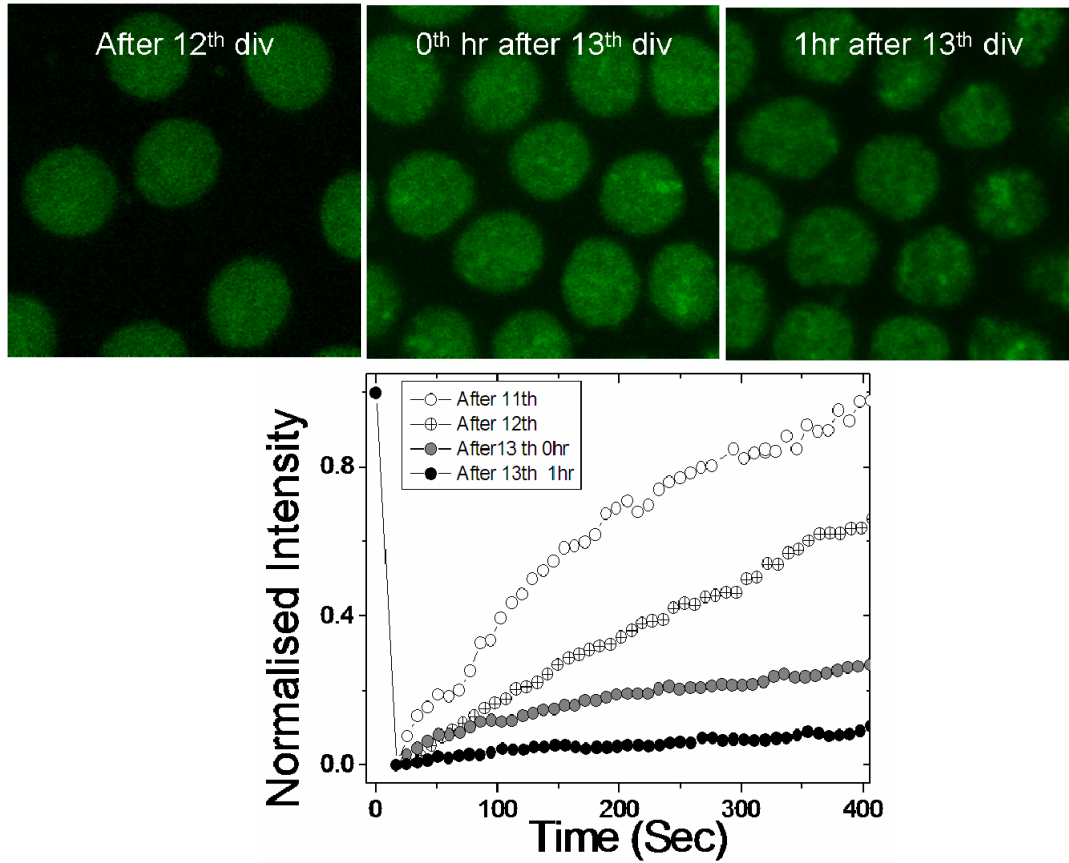
Figure 3.3.3.5 shows the results of the FRAP experiments of the whole cell nucleus in a developing *Drosophila* embryo, before cellularization. In *Drosophila* embryo, the cellularization starts after 13th nuclear division, and completes within one hour after 13th division at 25° C. The fluorescence image of the cell nucleus reveal that the nuclear shape and size change significantly once the cellularization begins. Before cellularization, all nuclei are spherical in shape and have uniform size distribution. After 1 hr from 13th nuclear division, as the cellularization proceeds the cell nuclear shapes become asymmetric and nuclei acquire distinct size and shape depending upon its localization inside the embryo (**Figure 3.3.3.4**). In the FRAP experiments, a nucleus is photobleached completely in 3-D and the fluorescent images of same nucleus are acquired with optimum laser power. The number of fluorophores in the cell nucleus is obtained by quantifying the fluorescence images of each of these nuclei in the subsequent frames. The exchange of core histones (H2B-EGFP) through the nuclear pores is calculated by normalizing the fluorescent intensity of the whole nucleus, as shown in **Figure-3.3.3.5**. From the **Figure-3.3.3.5**, it is clear that before cellularization, the rate of exchange of the core histones through the nuclear pore decreases significantly and after cellularization (1 hour after the end of 13th nuclear division) it reaches a minimal recovery, as expected. Since there is no significant gene expression till the beginning of 14th mitotic cycle, FRAP data indicate that maternally expressed core histones play a vital role in maintaining the chromatin organization before cellularization.

Figure 3.3.3.4



(a) Image of the different nuclei before and after cellularization and the respective threshold images. (b) The area and circularity of the nuclei before (0hr) and after cellularization (1hr). A significant decrease in nuclear area and circularity is an indicator of the cellularization.

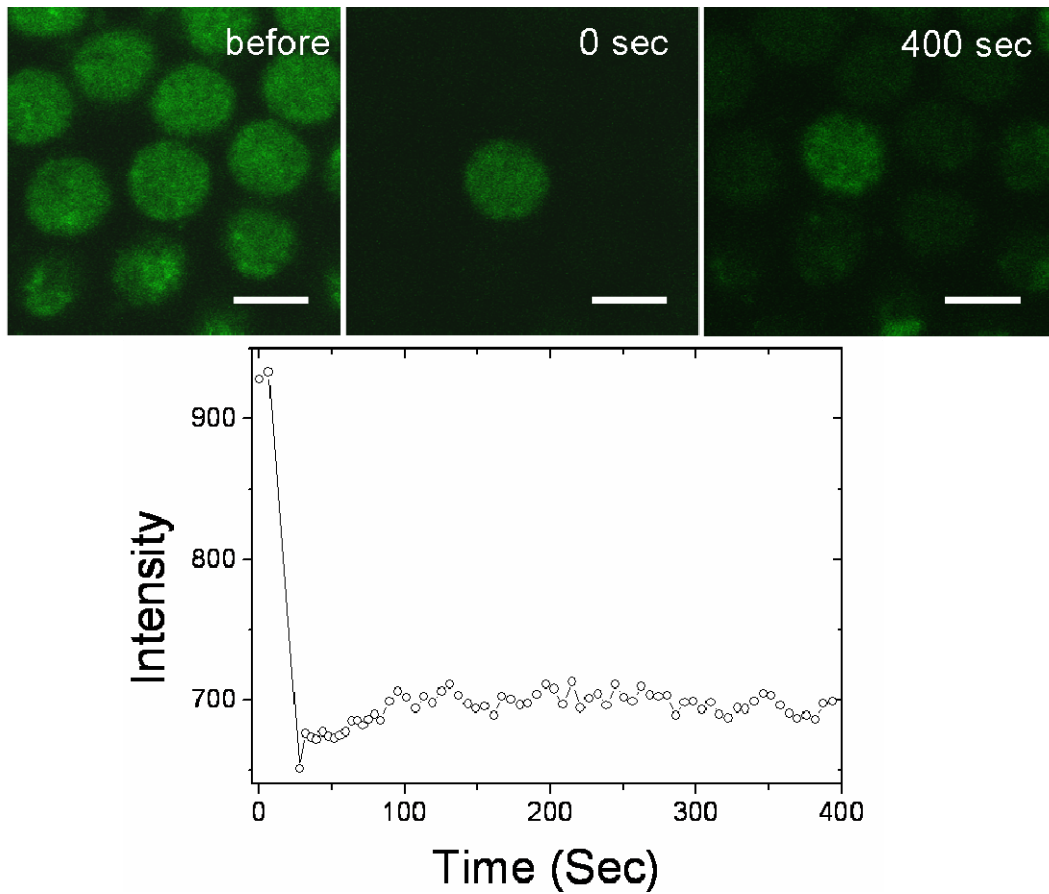
Figure 3.3.3.5



Subsequent frames of the confocal fluorescence images of *Drosophila* nucleus before cellularization are presented here. The cell nucleus before photobleaching and subsequent frames after photo bleaching (0 sec, 200 sec, and 400 sec) are shown above. The quantified normalized fluorescence intensities of the cell nucleus at different time points, after 11th, 12th and 13th nuclear division and 1 hrs from 13th nuclear division, are shown. Scale bar is ~5 μ m.

Our earlier FRAP experiments show that there is a significantly higher recovery of the core histones inside the cell nucleus before cellularization. It is not clear whether this exchange of the core histones is between the nucleus and the yolk or, between the adjacent nuclei. To understand the mechanism of core histone transport inside the nucleus, a FLIP experiment (Fluorescence loss in photobleaching) was carried out. In order to understand the fluorescence loss of the targeted nucleus and the resulting fluorescent gain of the adjacent photobleached nuclei, all the adjacent nuclei in the frame except the targeted nucleus are photobleached and followed in time. Experimental results indicate that, after photo bleaching, the intensity of all the adjacent nuclei increase but the intensity of the unbleached nucleus do not change, as shown in the **figure 3.3.3.6**. The FLIP experiment clearly indicates the exchange of the core histones between the embryonic yolk and the nuclei.

Figure 3.3.3.6

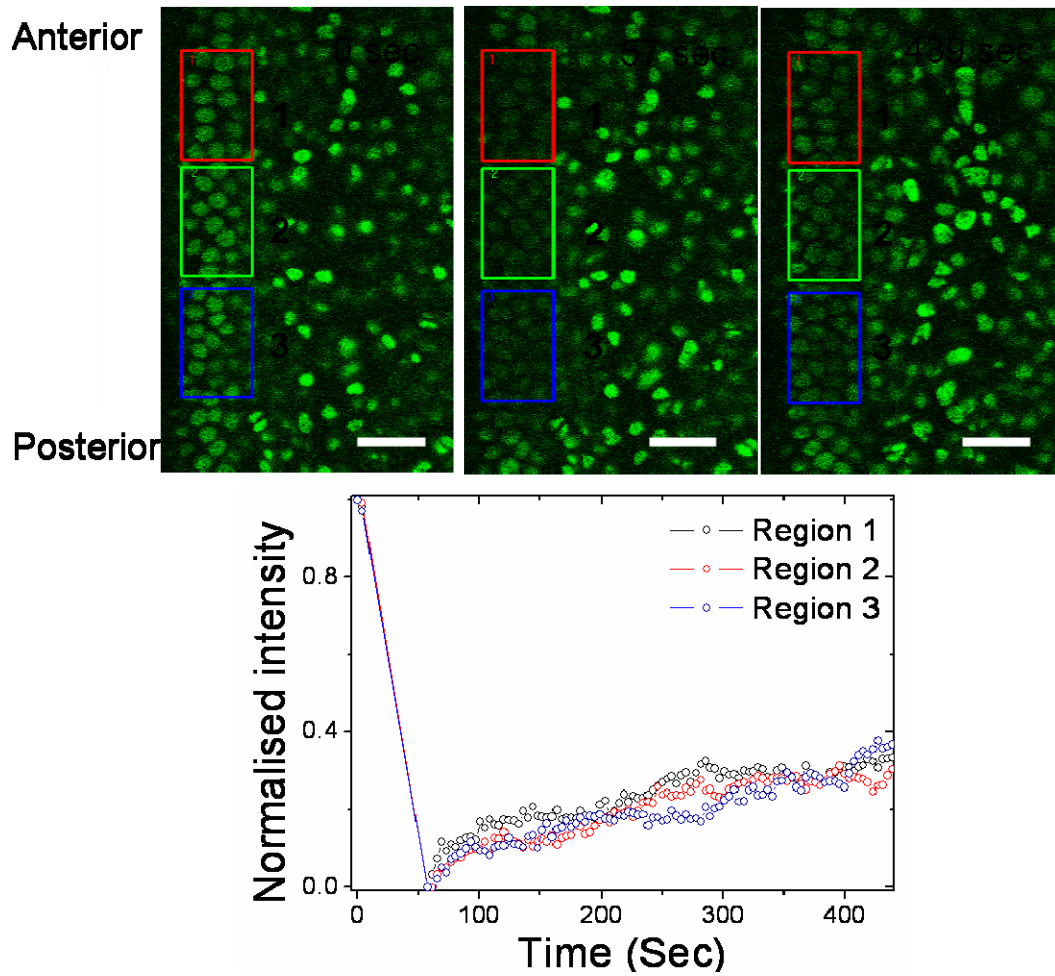


FLIP images after 13th nuclear division (before cellularization) of *Drosophila* embryo development. Quantified fluorescence intensity indicates no fluorescence loss in the targeted nucleus indicating the exchange of the core histones between the yolk and the nucleus. Scale bar ~5 μ m.

Time lapse fluorescence images show the flow of yolk from the posterior side to the anterior side in the earlier stages of *Drosophila* embryogenesis. This flow of the yolk is important to maintain the morphogen gradients in the early stages of embryogenesis. It is not clear whether the exchange of the core histones between the nuclei and yolk is also dependent upon the flow of yolk along the posterior to anterior axis. To understand the mechanism of core exchange, a long-strip bleaching experiment is performed along the anterior –posterior axis at different locations inside the embryo. After photo bleaching, the nuclei are followed. The quantitative intensities of different nuclei are obtained by image analysis. Our fluorescence recovery data (**figure 3.3.3.7**) indicate that the exchange of the core histones between the yolk and different nuclei is independent of the positioning of the nucleus as well as the direction of flow in the yolk.

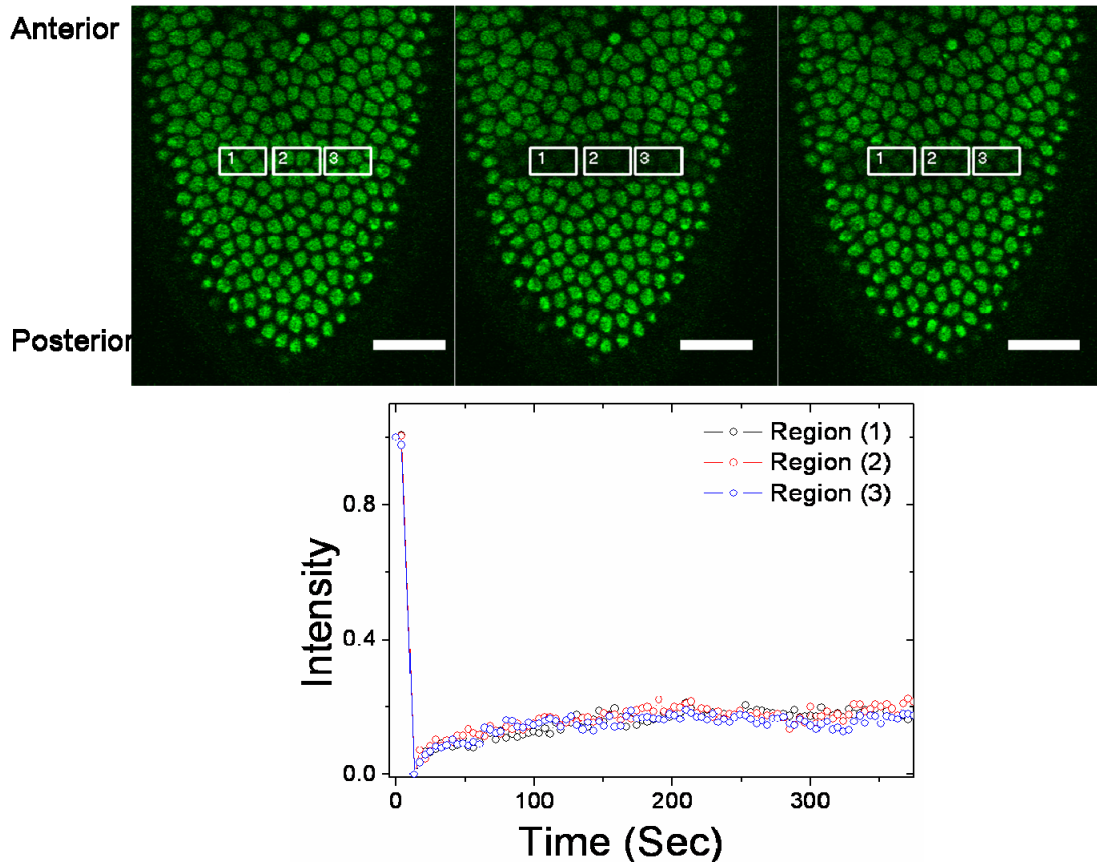
A strip photobleaching experiment was performed in the perpendicular direction from the anterior-posterior axis at different locations inside the early *Drosophila* embryo (**Figure 3.3.3.8**). Here again, the quantified fluorescence intensity at different locations along the strip indicates that the exchange is independent of the localization of the nucleus and the flow direction.

Figure 3.3.3.7



FLIP images after 13th nuclear division (before cellularization) of *Drosophila* embryo development. Quantified fluorescence intensity indicates that the exchange mechanism is independent of the flow direction. Scale bar ~5 μ m.

Figure 3.3.3.8



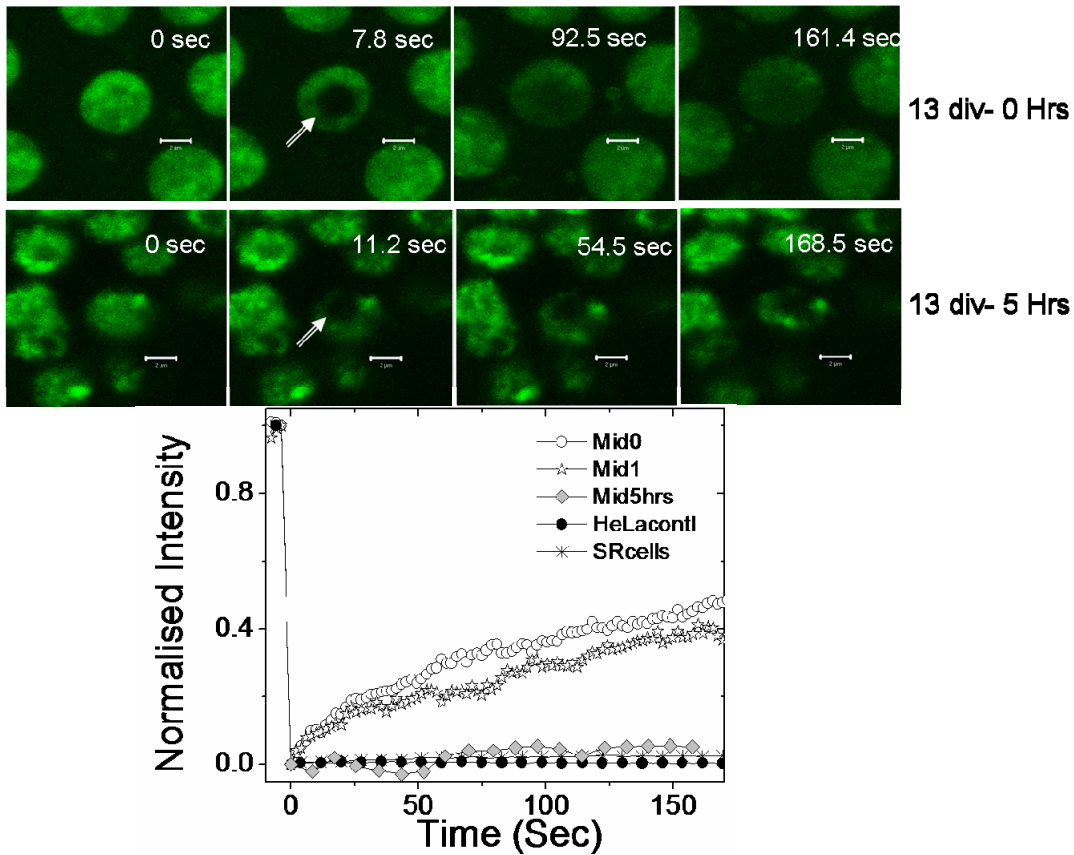
FLIP images after 13th nuclear division (before cellularization) along the perpendicular direction from anterior posterior axis of *Drosophila* embryo. Quantified fluorescence intensity indicates that the exchange mechanism is independent of the flow direction. Scale bar $\sim 5\mu\text{m}$.

3.3.1.2 Fluorescence recovery experiments indicate plasticity in chromosomal organization after cellularization.

Our FRAP and FLIP experiments on whole nuclei have shown higher exchange of the core histones between the nuclei and the embryonic yolk in the early part of development before cellularization. The FRAP data indicates that the exchange of the freely diffusing core histones completely stops after cellularization (1 hrs after 13th nuclear division). Therefore, to understand the exchange of the freely moving core histones with the bound histones inside the cell nucleus after cellularization, FRAP measurements are done in a small region inside the nucleus. From these measurements, the typical percentage of the bound and unbound population of the core histones in that particular area is obtained.

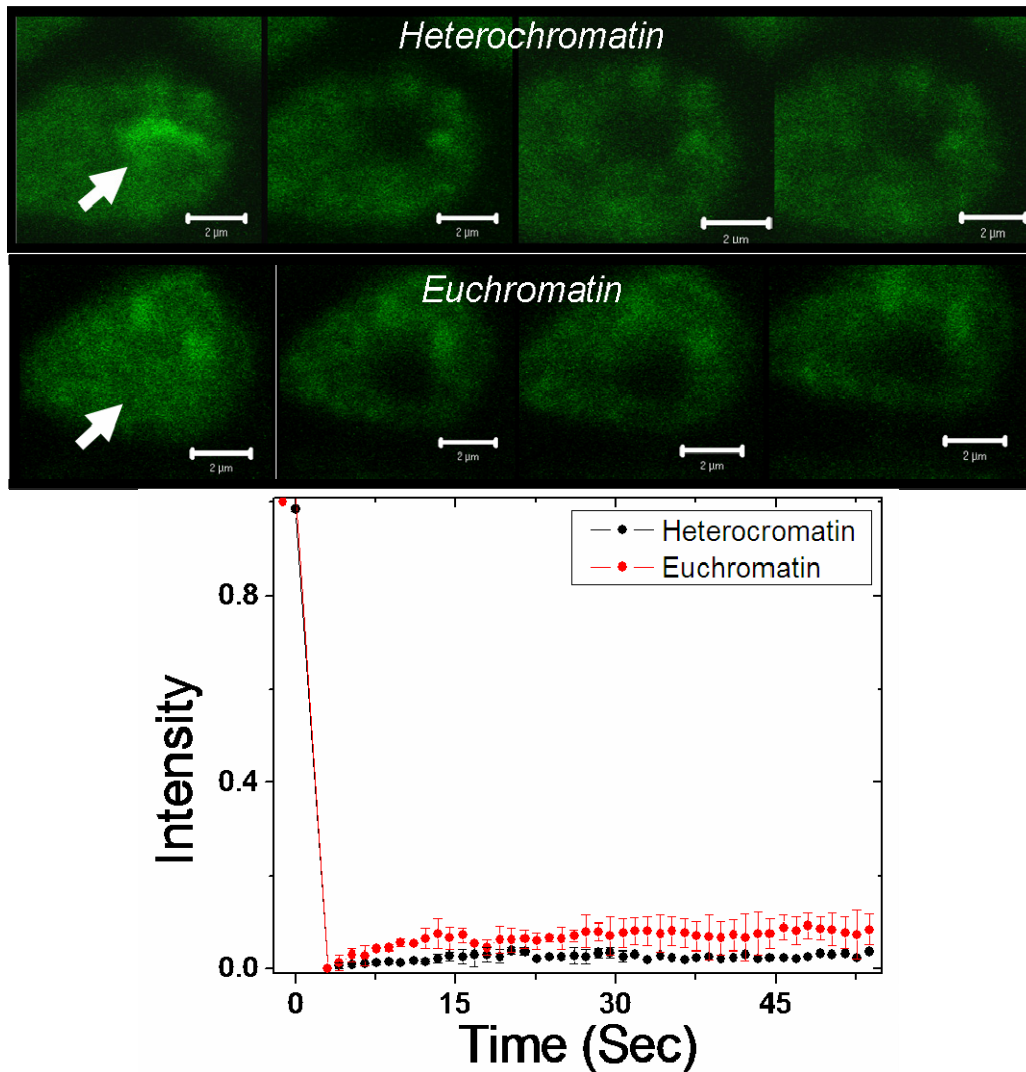
A small region inside the cell nucleus is photobleached after 13th nuclear division (0 hr), just after cellularization (after 1 hr from 13th nuclear division), and after 5 hrs from 13th nuclear division. Our fluorescence recovery data show significantly higher fluorescence recovery even after cellularization (1 hr from 13th nuclear division). Our FRAP data in the nuclei of differentiated cells, like HeLa nucleus, or *Drosophila* SR+ cells indicate negligible fluorescence recovery in the similar timescale under similar acquisition settings. It is known that the exchange mechanism of the core histones is very slow (<20% in ~30 min timescale) compared to the linker histones or non-interacting proteins like EGFP. As shown in the **Figure- 3.3.3.9**, ~40% fluorescence recovery in ~150 sec timescale for the core histones (H2B-EGFP) in the earlier part of *Drosophila* nucleus, even after cellularization, indicate chromosomal plasticity. After ~5 hrs from cellularization, the chromosomal structure becomes well defined and gets a differentially compacted structure inside the cell nucleus.

Figure 3.3.3.9



Fluorescence recovery after photobleaching curves in the small region inside the cell nucleus at different time points of embryonic development. FRAP data indicate a high fluorescence recovery in the nuclei after 0 hrs from 13th nuclear division and even after 1hr from 13th nuclear division (After completion of cellularization). FRAP data indicate a negligible fluorescence recovery inside the nucleus after 5hrs from 13th nuclear division, which is comparable to the FRAP recovery of the core histone (H2B-EGFP) in the differentiated cells, HeLa nucleus and *Drosophila* SR⁺ cells.

Figure 3.3.3.10



Confocal fluorescent images of the nucleus before and after photobleaching both in the euchromatin and heterochromatin regions. The FRAP recovery curve indicates negligible recovery in the both the spaces indicating the condensed chromosomal compaction in both euchromatin and heterochromatin regions (5 hrs from 13th nuclear division).

Confocal fluorescent images show distinct patches of condensed chromatin structure in the nucleus at 5hrs from 13th nuclear division stage of embryonic development. The FRAP curves show minimal fluorescence recovery both in the euchromatin and heterochromatin regions as detailed in **Figure 3.3.3.10**.

3.3.1.3 Freely diffusing core histones are in multimeric form inside the cell nucleus as well as in the yolk before cellularization

Our earlier experiments on core histone diffusion inside the HeLa cell nucleus show that the core histones are in multimeric form inside the HeLa cell nucleus whereas in the cytoplasm of an over-expressing cell the core histones are in monomeric form.

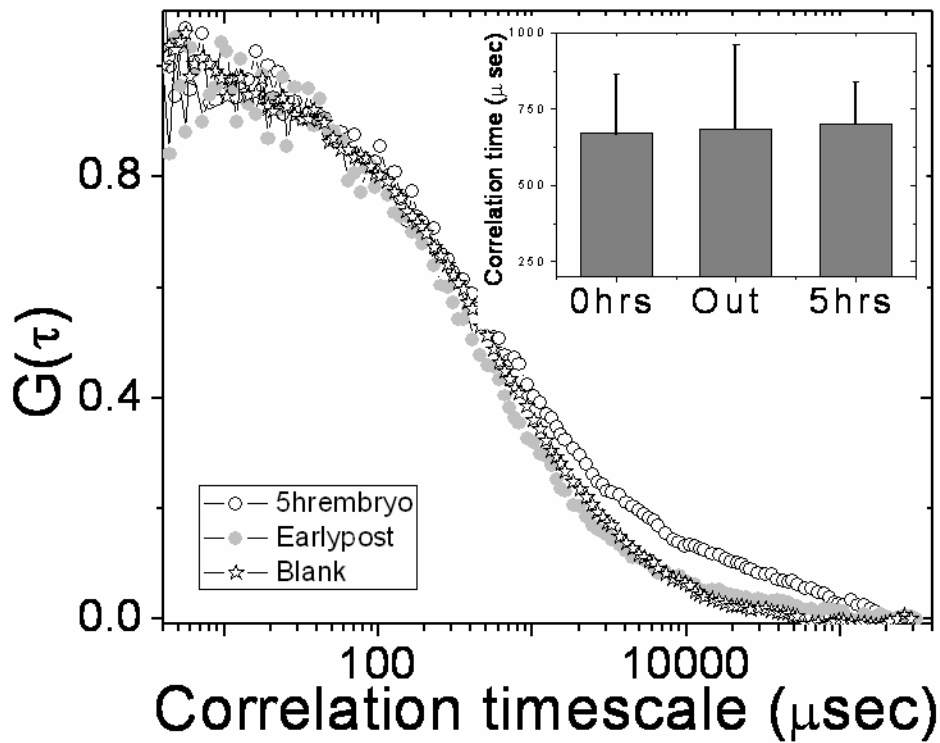
To understand the state of the freely diffusing core histones in the developing *Drosophila* embryo, a fluorescence correlation spectroscopy experiment is carried out. The autocorrelation timescale obtained from the autocorrelation curve indicate that the diffusion timescales of the core histones (H2B-EGFP) is significantly slower compared to the expected monomeric core histones. The typical correlation timescales obtained for the core histones (H2B-EGFP) are, $\sim (669.8 \pm 193.4) \mu\text{sec}$ inside the cell nucleus before cellularization (0 hr after 13th nuclear division), $\sim (684.1 \pm 277.3) \mu\text{sec}$ in the yolk before cellularization (0 hr after 13th nuclear division) and $\sim (701.8 \pm 136.1) \mu\text{sec}$ in the cell nucleus after 5 hr from 13th nuclear division, as shown in the **Figure 3.3.3.11**. The timescale of diffusion for the core histones in the early embryo, both in the cell nucleus and as well as in the yolk indicate that the multimeric core histones are exchanged between the nuclei and in the yolk. In the early embryo, the maternally expressed core histones are in the multimeric form, and the higher exchange of these multimeric core histones from the yolk to the cell nucleus may be important to maintain the epigenetic state of the cell nucleus.

The autocorrelation function curves obtained for the multimeric core histones inside the nucleus in the experimental time points, (0 hr after 13th nuclear division and 5 hrs after 13th nuclear division) do not fit with the single species purely

diffusive autocorrelation function. Fitting the correlation curve with the single species diffusive correlation curve with β (a scaling parameter defining the sub-diffusive behavior) as a free parameter, it is found the correlation curve fits well with β less than 1, indicating a sub-diffusive transport. The mean β value for the core histones has been used to estimate the heterogeneity in the chromosomal mesh structure in the nucleus before cellularization (0hr after 13th nuclear division) and after 5hrs from 13th nuclear division. Confocal fluorescence images of the cell nucleus (**Figure 3.3.3.12**) show that the nuclear shape changes and distinct heterogeneous chromosomal compaction after 5 hrs from 13th nuclear division. The distribution of β factor in the nucleus at 0 hr after 13th nuclear division and after 5hrs from 13th nuclear division show that after cellularization, the chromosomal compaction changes to a heterogeneous compaction stage giving rise to a lower β . The mean β factor obtained over 30 such nuclei, the β factor is $\sim (0.82 \pm 0.08)$ for the nuclei at 0hr after 13th nuclear division, whereas the β changes to $\sim (0.71 \pm 0.08)$ inside the nucleus after 5 hrs from 13th nuclear division.

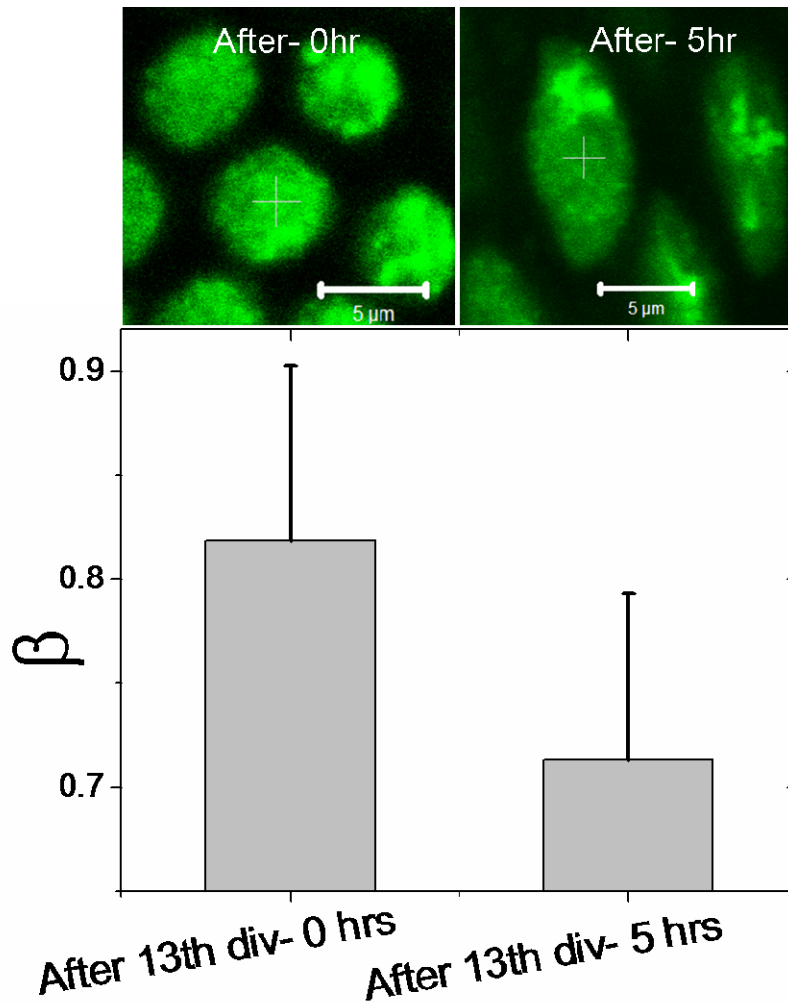
The distinct patches in the fluorescent images of the nucleus and the change in β factor indicate the origin of a distinct heterogeneous chromosomal compaction in the nucleus after the beginning of cellularization in the early stages of *Drosophila* embryonic development.

Figure 3.3.3.11



Representative autocorrelation curves for the core histone (H2B-EGFP). The correlation curves indicate that the core histones follow sub-diffusive transport inside the cell nucleus, both after 0hrs from 13th nuclear division and 5hrs from 13th nuclear division. Typical correlation timescale indicates the core histones are in multimeric form inside the cell nucleus as well as in the yolk before cellularization. The mean and the standard deviation of the correlation timescales for H2B-EGFP (0hrs after 13th nuclear division, 5 hrs after 13th nuclear division, and in the yolk after 0hrs from 13th nuclear division) are shown in the inset. (n=30)

Figure 3.3.3.12



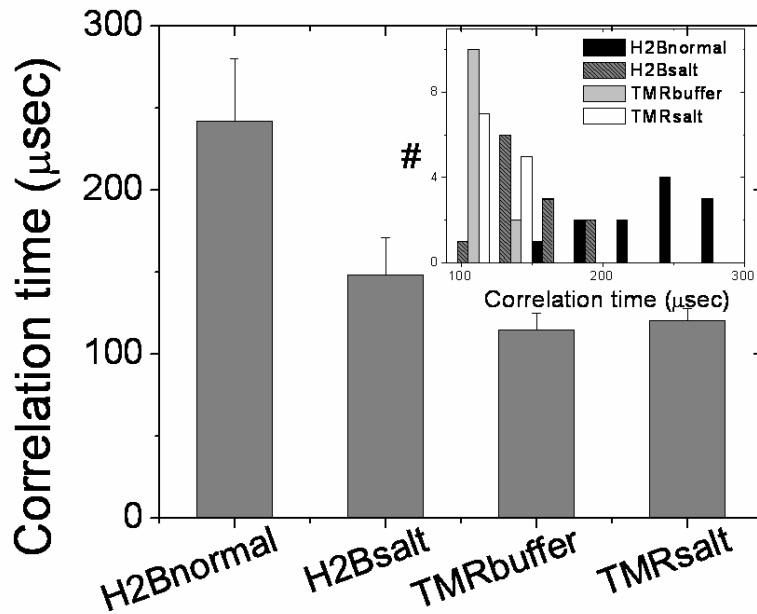
Confocal fluorescence images of the nuclei after 0 hrs from 13th nuclear division and 5hrs after 13th nuclear division .Images indicate the heterogeneous patches of chromatin condensation after 5 hrs from 13th nuclear division. The mean and the standard deviation of β factor inside the cell nucleus after 0hrs from 13th nuclear division and 5hrs from 13th nuclear division are shown in the figure. The decrease in β factor indicates the beginning of heterogeneous compaction state of the nucleus after 5hrs from 13th nuclear division. (n=30)

To understand whether the maintenance of the multimeric form of the core histone requires an embryonic environment, a FCS experiment was carried out on the embryonic extract from the embryos at a very early stage of development (Before 11th nuclear division). The protocol for preparing embryo-extract is detailed below, 50 early embryos were placed in a micro-centrifuge tube and crushed. 100 μ l PBS was added into it before spinning at 12,000 rpm for 4 minute. The supernatant was collected for further experiments. 2 μ l of \sim 10 μ M TMR-dextrans was added and used in the FCS measurement.

FCS measurement was done using 488nm line (for H2B-EGFP) and 543nm line (for TMR-dextrans) of Ar-ion laser. The mean correlation timescale obtained for H2B-EFP diffusion is (242 \pm 38) μ sec whereas the correlation timescale for TMR-dextrans is (115 \pm 10) μ sec. The correlation timescale for H2B-EGFP diffusion is significantly slower than the expected correlation timescale of the monomeric H2B-EGFP. To validate the data, a 40 μ l concentrated (2M) NaCl solution is added into the mixture and FCS experiment is done in the mixture. The mean correlation timescale obtained in the salt buffer for H2B-EFP diffusion is (143 \pm 23) μ sec whereas the correlation timescale for TMR-dextrans is (120 \pm 7) μ sec, as shown in the **Figure 3.3.3.13**.

The mean correlation timescales indicate the existence of multimeric core histones in the buffer. After addition of salt, the multimeric H2B-EGFP becomes monomeric, though the TMR-dextrans diffusion data indicates the concentration of the medium is not changed upon salt treatment. The experimental data indicates that the core histones preserve their multimeric form even outside the embryonic environment.

Figure 3.3.3.13



The mean correlation timescale for the core histones (H2B-EGFP) (extracted from the embryonic yolk) in physiological buffer (PBS) and in high salt concentration. The mean correlation timescale of the core histones in these two conditions are compared with the correlation timescale for 10kD TMR-dextran under similar conditions. Inset shows the distribution of timescales.

3.3.3.4 Diffusion mobility of the linker histones inside the early *Drosophila* embryo

To understand the diffusive mobility of the linker histones inside the *Drosophila* embryo, Alexa-488 labeled linker histones were microinjected inside the early embryo. Wild type *Drosophila* flies were kept in a sucrose plate for 1hr for egg-laying, after which they were collected for micro-injection.

From the fluorescence images, shown in the **Figure- 3.3.3.14**, it is clear that the linker histones labeled with Alexa-488 properly localize inside the nucleus and mark the chromosome. The incorporation of Alexa-488 labeled linker histone into

the nucleus does not alter the mitotic cycle in the early embryo, when compared with the *Drosophila* embryo where core histone (H2B) is genetically tagged with EGFP (H2B-EGFP). Fluorescence images indicate that the chromosomal localization of the Alexa-488 labeled linker histones are also maintained through mitotic division **Figure- 3.3.3.14**.

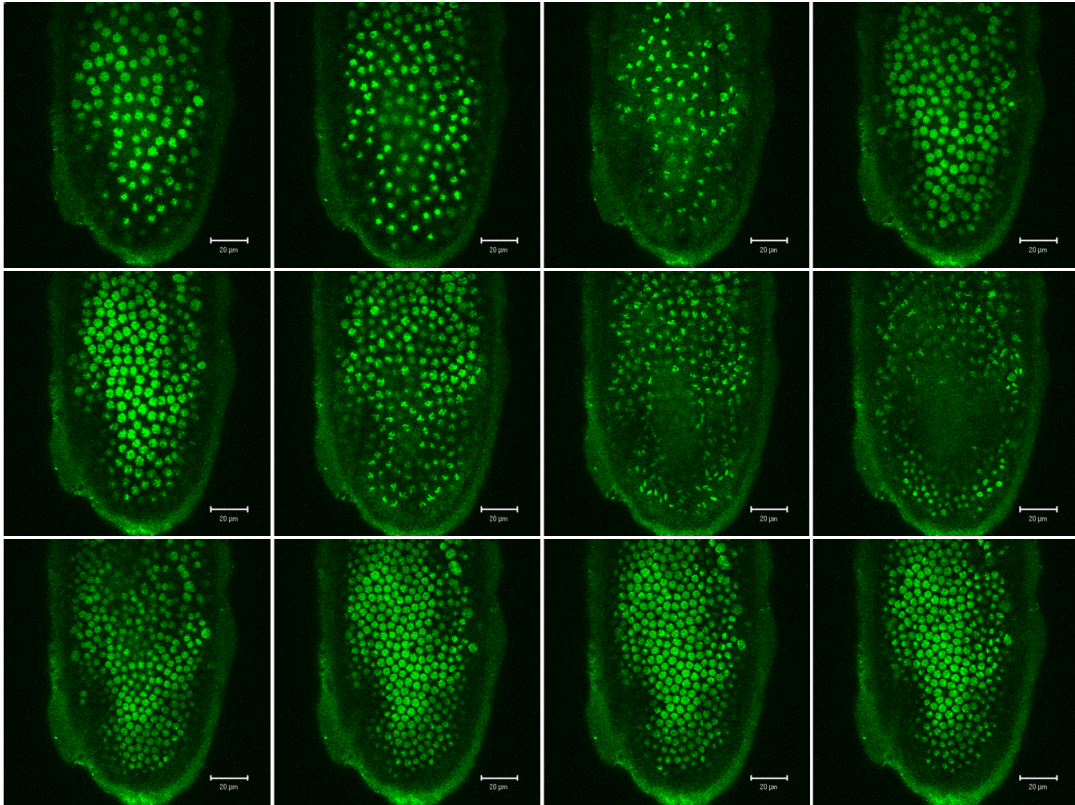
The Alexa-488 labeled linker histones in the *Drosophila* embryo are used for the spectroscopic measurements. Here the embryonic development was followed in time and FRAP experiments are done after 12th nuclear division.

(i) Higher exchange of the linker histones between nuclei and the yolk in the early *Drosophila* embryo before cellularization

The previous study shows that a large amount of core histone exchange takes place between the nuclei and the yolk before cellularization, Hence we microinjected Alexa-488 labeled linker histones into the *Drosophila* embryo and tried to understand the exchange mechanism of the linker histones between the nuclei and the yolk. In this experiment, nuclei are followed through 12th and 13th nuclear division and the incorporation of the linker histones in the chromatin fibers is observed. In the FRAP experiment, a nucleus is photobleached completely and followed with time. The images show (**Figure-3.3.3.15**) a significant exchange of the linker histones, like the core histones, in the early embryo before cellularization.

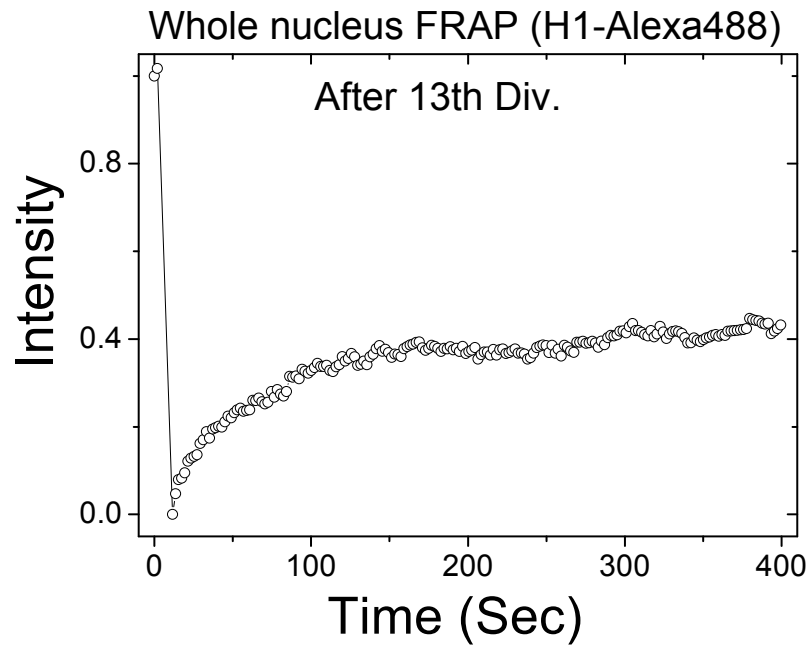
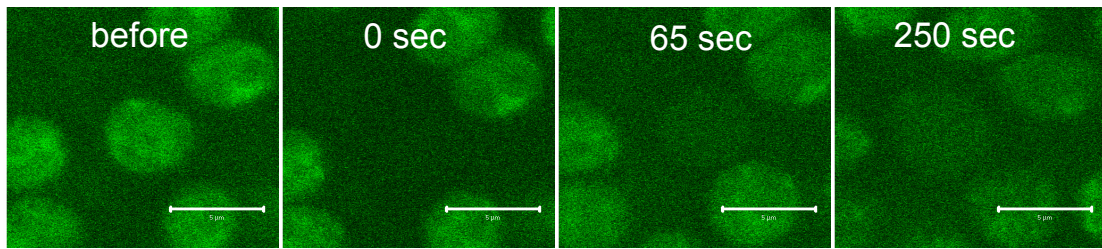
Figure 3.3.3.14

Linker Histone (H1-Alexa488) injected embryo development



Nuclear localization of Alexa-488 labeled linker histone in the *Drosophila* early embryo. Chromosomal localization of the linker histones (Alexa-488 labeled) is also maintained during different nuclear division.

Figure 3.3.3.15

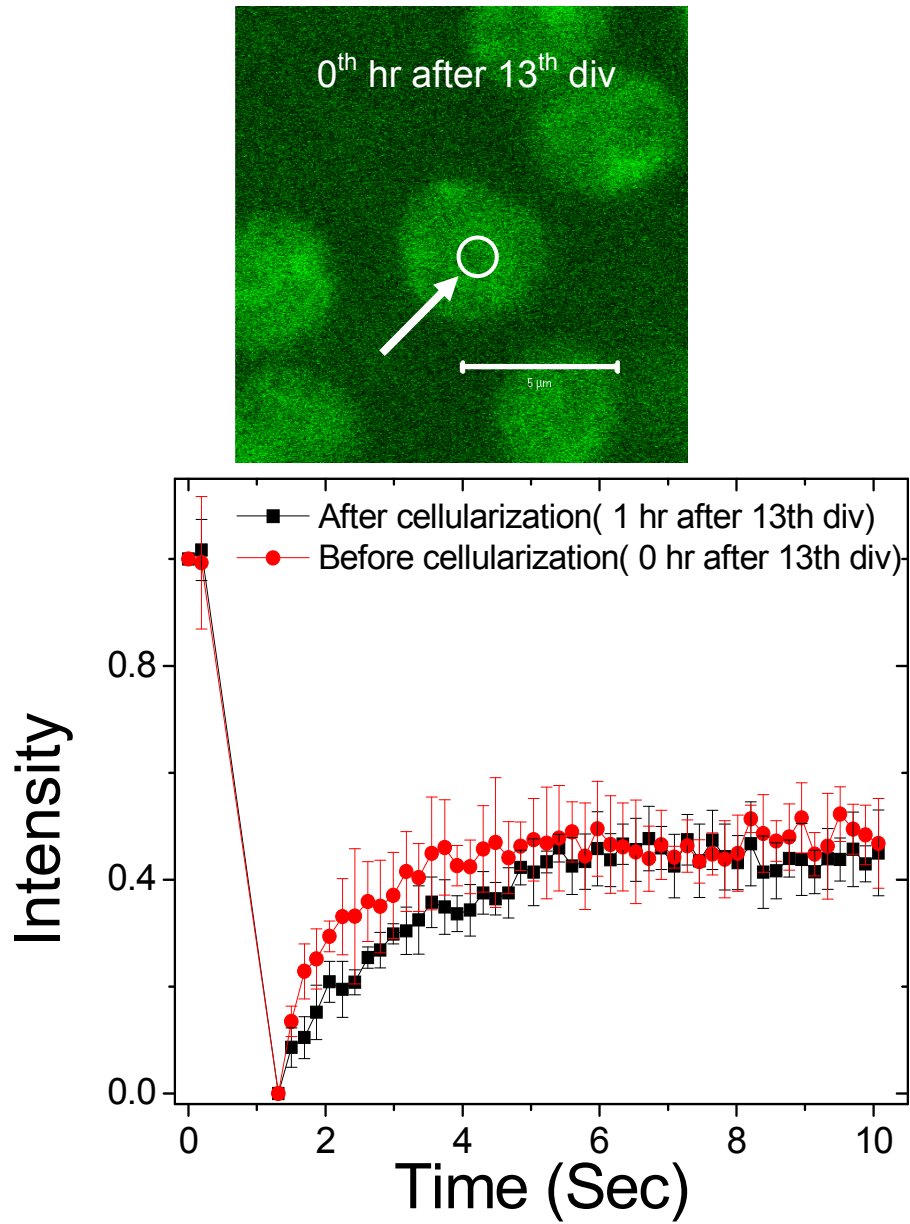


Subsequent frames of fluorescence recovery after photobleaching of the linker histones (labeled with Alexa-488) indicates quantified normalized fluorescence intensities of the cell nucleus at different time points, after the beginning of 0th hr from 13th nuclear division. Scale bar is ~5 μm.

(ii). Higher exchange of the bound and unbound linker histones is observed in the early *Drosophila* embryo even after cellularization.

The earlier part of this work has shown that there is plasticity in the chromosomal compaction state in the early part of development at the nucleosomal level. It is known that the linker histones stabilize the higher order chromosomal structure. We therefore tried to calculate alterations in the interaction timescales of the linker histones with the chromatin fiber in the early part of development. To address this, a FRAP experiment of linker histones, tagged with Alexa-488, was done in the early embryo after 0hrs and 1hrs from 13th nuclear division in a developing embryo. In this experiment, a ~1.4 μm diameter area is photobleached and the fluorescence recovery curves even after cellularization indicate a faster recovery timescale compared to the recovery timescale observed for EGFP tagged linker histones in a somatic cell nucleus (HeLa cells). **(Figure 3.3.3.16)**

Figure 3.3.3.16

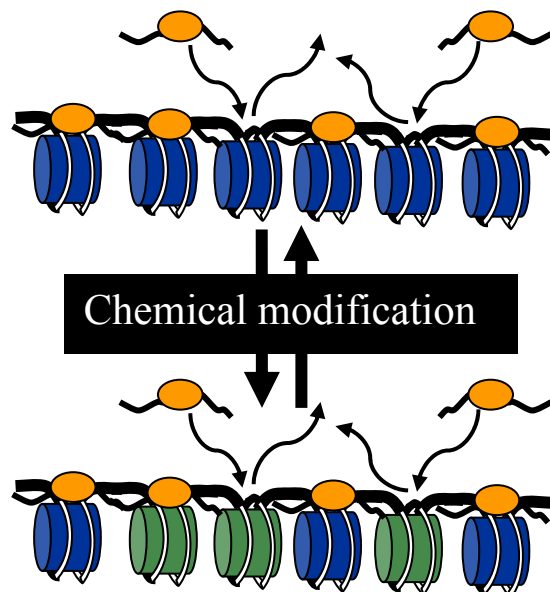


FRAP recovery data for the linker histones labeled with Alexa-488. Data indicate that linker histone recovery is much faster, even after cellularization, compared to that in the interphase cells (HeLa cells).

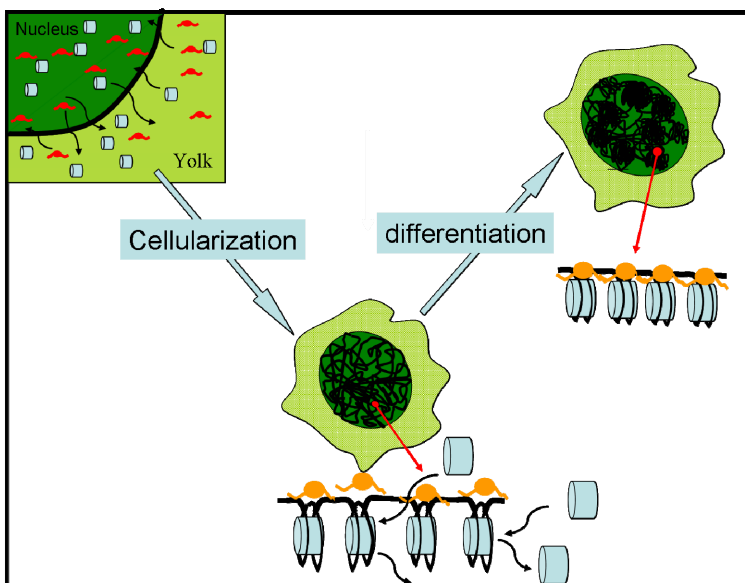
3.4 Conclusion

At the inception of this thesis work I established that freely diffusing core histones are in multimeric form, and linker histones display unique binding-unbinding characteristics in relation to the chromatin fiber, in the nuclei of live cells. In this context it became important to interrogate these properties under conditions of global changes in chromatin structure. I thus studied histone diffusion in TSA treated cells, where due to the presence of higher fractional acetylated histones the chromatin undergoes drastic decompaction. From fluorescence correlation spectroscopy experiments I observed that even under these conditions the freely diffusing core histones remain in the multimeric form inside the HeLa nucleus. In our FRAP studies on H1.5-EGFP expressing cells, higher levels of fluorescence recovery was observed, probably due to the higher expression of linker histones. Interestingly FCS data from similar cells indicated that due to chemical modification of the core and the linker histones, the interaction timescale of linker histones (H1.5-EGFP) increases in the TSA-treated cells compared to the control cells.

Our diffusion mobility data indicate the direct correlation of the diffusion and interaction of the core and the linker histones with the chemical modification of the chromatin fiber.



In a second condition of global changes in chromatin structure, I monitored the evolution of histone dynamics in early *Drosophila* embryo development. Using transgenic fly embryos where the histone H2B is genetically tagged to EGFP, and by microinjecting fluorescently labeled linker histones into the *Drosophila* embryo, I studied the diffusion behavior of core and linker histones, the exchange of these proteins with the chromatin fiber and the transport of these proteins through the nuclear pore before and after cellularization in a developing fruit fly embryo. I observed a high degree of exchange of the multimeric core histones through the nuclear pore before cellularization. As the embryo proceeds from 11th to 13th nuclear division, the exchange rate also decreases significantly and vanishes completely after cellularization. Fluorescence recovery data for both the core and the linker histones indicate chromosomal plasticity in early development even after cellularization. After ~5 hrs from cellularization, the chromosomal structure becomes well defined and acquires a differentially compacted structure inside the cell nucleus. The phenomenon is observed both in the euchromatin regions and heterochromatin regions after 5 hrs from 13th nuclear division. Thus we demonstrate a direct connection between the state of differentiation of the cells, and the structure of the chromatin.



3.5 Reference

1. Wang, Y., et al., *Beyond the double helix: writing and reading the histone code*. Novartis Found Symp, 2004. 259: p. 3-17; discussion 17-21, 163-9.
2. Rupp, R.A. and P.B. Becker, *Gene regulation by histone H1: new links to DNA methylation*. Cell, 2005. 123(7): p. 1178-9.
3. Meshorer, E., et al., *Hyperdynamic plasticity of chromatin proteins in pluripotent embryonic stem cells*. Dev Cell, 2006. 10(1): p. 105-16.
4. Meshorer, E. and T. Misteli, *Chromatin in pluripotent embryonic stem cells and differentiation*. Nat Rev Mol Cell Biol, 2006. 7(7): p. 540-6.
5. Fu, G., et al., *Mouse oocytes and early embryos express multiple histone H1 subtypes*. Biol Reprod, 2003. 68(5): p. 1569-76.
6. Saeki, H., et al., *Linker histone variants control chromatin dynamics during early embryogenesis*. Proc Natl Acad Sci U S A, 2005. 102(16): p. 5697-702.
7. Fan, Y., et al., *H1 linker histones are essential for mouse development and affect nucleosome spacing in vivo*. Mol Cell Biol, 2003. 23(13): p. 4559-72.
8. Fan, Y., et al., *Individual somatic H1 subtypes are dispensable for mouse development even in mice lacking the H1(0) replacement subtype*. Mol Cell Biol, 2001. 21(23): p. 7933-43.
9. Toth, K.F., et al., *Trichostatin A-induced histone acetylation causes decondensation of interphase chromatin*. J Cell Sci, 2004. 117(Pt 18): p. 4277-87.
10. Yellajoshiyula, D. and D.T. Brown, *Global modulation of chromatin dynamics mediated by dephosphorylation of linker histone H1 is necessary for erythroid differentiation*. Proc Natl Acad Sci U S A, 2006. 103(49): p. 18568-73.

11. Bhattacharya, D., et al., *EGFP-tagged core and linker histones diffuse via distinct mechanisms within living cells*. *Biophys J*, 2006. 91(6): p. 2326-36.